Contents list available at CBIORE journal website

International Journal of Renewable Energy Development

Journal homepage: https://ijred.cbiore.id

Research Article

Effect of various silica-supported nickel catalyst on the production of bio-hydrocarbons from oleic acid

Rafly Riyandi[a], Nino Rinaldi[b], Rika Tri Yunarti[c], Adid Adep Dwiatmoko[b*], Fidelis Stefanus Hubertson Simanjuntak[a*]

[a]*Department of Renewable Energy Engineering, Universitas Prasetiya Mulya, BSD City Kavling Edutown I.1, Tangerang, Indonesia*

[b]*Research Center for Chemistry, National Research and Innovation Agency (BRIN), Gd. 452 Kawasan PUSPIPTEK Serpong, Tangerang Selatan, Indonesia*

[c]*Research Department of Chemistry, Faculty of Mathematics and Natural Sciences, Universitas Indonesia, Depok, West Java 16424, Indonesia*

Abstract. The conversion of fatty acids into bio-hydrocarbons can be carried out through a deoxygenation (DO) reaction. Catalytic deoxygenation of fatty acids can occur through three reaction pathways: decarbonylation, decarboxylation, and hydrodeoxygenation. In this study, three kinds of silica were prepared: (i) silica obtained from the rice husk ash (RHA); (ii) synthetic mesoporous silica SBA-16; and (iii) commercial silica. All prepared silica was used as supported nickel (Ni) catalyst for bio-hydrocarbon production through DO reaction of oleic acid. The objective of this study was to investigate the effect of variations of silica on the reaction pathway and final products composition of DO reaction of oleic acid. The catalysts were characterized by X-ray fluorescence (XRF), X-ray diffraction (XRD), surface area analysis, and NH_3-temperature-programme desorption. Based on XRF and XRD analysis results, it can be concluded that nickel was successfully impregnated into all silica. All samples of catalysts were used in a reaction carried out at temperature of 285 °C under a pressure of 40 bar H_2 for 2h. The results showed that all catalysts were able to convert oleic acid to bio-hydrocarbon with differences in products composition. The highest oleic acid conversion of 98.25% was achieved with Ni/RHA catalyst but the obtained liquid products was the lowest among other catalysts. It is found that this phenomenon was closely related to the acidity properties of the catalyst.

Keywords: Bio-hydrocarbon, green diesel, Ni/Silica catalyst, deoxygenation, fatty acid

Received: 18th Dec 2023; Revised: 6th March 2024; Accepted: 15th April 2024 ; Available online: 30th April 2024

1. Introduction

Indonesia is the largest palm oil producer in the world. Today, palm oil is used in Indonesia as cooking oil and biodiesel raw material. With the large potential of palm oil in Indonesia, it is important to find ways to utilize palm oil in order to increase its economic value. Palm oil is a vegetable oil that contains fatty acids and can be used as raw material for producing hydrocarbon fuels. The fatty acid that is most abundant in palm oil is oleic acid, which is 45.02% in crude palm oil (CPO) and 76.27% in refined palm oil (RPO) (Muanruksa *et al*., 2021).

Oleic acid can be converted into bio-hydrocarbon with high yields through the deoxygenation process. The various possible mechanisms for deoxygenation include (i) decarboxylation ($deCO_2$) which removes the carboxyl group to produce alkanes and CO_2; (ii) decarbonylation (deCO) which produces alkenes, CO, and H_2O; and (iii) hydrodeoxygenation (HDO) which involves breaking the C–O bond with hydrogen to produce alkanes and H_2O from fatty acids, involves reducing the oxidation number of the carbon atom of the carboxylate group using H_2 (Oi *et al*., 2016). The deoxygenation process allows the production of compounds with low oxygen content. Low oxygen content in fuel can reduce corrosion properties and increase combustion efficiency by increasing the heating value (Ooi *et al*., 2019).

Many researches have been done on silica as catalyst support because of its unique properties. Silica has large surface area, large pore volume, and regular pore structure (Takahashi *et al*.). MCM-41 and SBA-15 are the two most common types of mesoporous silica nanoparticles (Katiyar *et al*., 2016). SBA-15 nanoparticles created by combining tetraethyl orthosilicate as silica source with a structure directing agent, called Pluronic P123. After calcination, nano-sized spheres or rods are formed, containing a uniform arrangement of pores. The shape of the silica and the pores produced can be altered by using various structure directing agents. The advantage of mesoporous SBA-15 as catalyst support is their large surface area, tunable pore diameter (4–30 nm) and thick pore walls (Chaudhary and Sharma, 2017). In addition, Ni with a mesoporous silica support catalyst has advantages because many studies show that the Ni/SBA-15 catalyst successfully achieves high dispersion of nickel on the support and a stable condition in the pores thereby minimizing sintering and coke formation (Karam and El Hassan, 2018). An alternative source of silica is rice husk which is agricultural waste that are abundantly available in Indonesia. Rice husk is composed of 70%-80% lignocellulose and 20%-30% inorganic compound. SiO_2 is the major constituent of inorganic

* Corresponding author
Email: adid001@brin.go.id (A.A.Dwiatmoko); fidelis.simanjuntak@prasetiyamulya.ac.id (F.S.H.Simanjuntak)

https://doi.org/10.61435/ijred.2024.60054
ISSN: 2252-4940/© 20xx.The Author(s). Published by CBIORE

compound, approximately in the range of 85%–95% (Park *et al*., 2021; Ogwang *et al*., 2021). Rice husk ash (RHA) has been widely developed as an adsorbent for removal of organic dye pollutant i.e methylene blue, indigo carmine dye, and also for removal of heavy metal ions, such as Pb^{2+} and Cd^{2+}. A few research groups have studied the utilization of RHA as catalyst support in chemical reaction, such as transesterification of soybean oil for biodiesel production, hydrogen production from ethanol steam reforming, dehydrogenation of ethanol to acetaldehyde, and CO_2 methanation for CH_4 production (Chen *et al*., 2013; Wang *et al*., 2019; Chang *et al*., 2006; Pavioti *et al*., 2020).

Nickel-based catalysts have good capabilities in deoxygenation reactions. The surface character of Ni metal functions as a trap for hydrogen bonding which reduces the activation energy of hydrogen dissociation (Liu *et al*., 2013). In addition, the metallic properties of Ni can cause reactions similar to those of noble metals (palladium or platinum), such as breaking C-C or C-H bonds for hydrocarbon reactions (De *et al*., 2016). Nickel oxide reduction plays an important role in heterogeneous catalytic reactions because Ni with zero oxidation state is the most active form in terms of surface adsorption ability, activation, and radical formation properties (Richardson *et al*., 2003; Syed-Hassan and Li, 2011). Several research groups have studied the use of nickel for bio-hydrocarbon production from vegetable oil. Kaewtrakulchai *et al*. reported that catalytic hydrocracking of palm oil with porous biochar supporting nickel phosphide exhibited 100% conversion of palm oil with majority hydrocarbon products, which was in the jet fuel range (Kaewtrakulchai *et al*.,2022). In addition, Liu, *et al*. (2015) have succeeded in applying the Ni-based catalyst to combine with various type of mesoporous silica support in HDO reaction and find conversion of castor oil or C16-C19 alkanes into high yields of bio-aviation fuel with high isomerization selectivity (Liu *et al*., 2015). Another study succeeded in converting palm fatty acid distillate into diesel-range hydrocarbons using Ni/SBA-15 as catalyst with high yield of 85.8% (Kamaruzaman *et al*., 2020). The same research group also reported hydrogen-free catalytic deoxygenation of waste cooking oil over various bimetallic catalyst-supported on SBA-15. The results showed Ni-Fe/SBA-15 exhibited the highest yield of liquid hydrocarbons (Rashidi *et al*.,2022).

To the best of our knowledge, there have been no studies comparing various silica materials as Ni catalyst support for deoxygenation reactions. Apart from that, the use of rice husk-derived silica as a catalyst support in deoxygenation reactions is still not widely used. This research aims to determine the effect of variations in silica as a nickel support catalyst on the production of bio-hydrocarbons from oleic acid. The variations of silica that were used are commercial silica (Comm), rice husk silica (RHA), and mesoporous silica (SBA-16).

2. Experimental

2.1 Materials

The chemicals used in this study were commercially available and used without further purification. hydrochloric acid (HCl), pluronic F127, sulfuric acid (H_2SO_4), eicosane, and oleic acid (technical grade, 90%) were purchased from Sigma-Aldrich, while silica gel 60 (commercial silica), tetraethyl orthosilicate (TEOS), nickel(II) chloride hexahydrate ($NiCl_2.6H_2O$), n-butanol, sodium hydroxide (NaOH), and dichloromethane (DCM) were purchased from Merck.

2.2 Catalyst preparation

Rice husk ash (RHA) is filtered using a 75-micron filter. 20 gr of RHA was dispersed in 100 ml of 2M HCl. After filtering, the RHA was stirred with 200 ml of 2.5M NaOH solution at 90 °C for 3 h. Pure silica can be extracted by the titration method using 5M H_2SO_4 solution with constant stirring under controlled conditions. Wash the silica gel and dry it at 105 °C for 5 h.

The preparation of SBA-16 materials was carried out using Pluronic F127 (triblock co-polymer - Sigma) and n-butanol as co-surfactant. 3.5 g of Pluronic F127 is mixed in 0.4 M HCl solution (175 mL) at a temperature of 45 °C. n-butanol (13 mL) was added to the mixture. After that, 16.7 g of TEOS (Tetraethyl orthosilicate, Acros Organics) was added while continuing to stir for 20 hours. Then, the final mixture was heated in an autoclave for 24 h at 98 °C. The precipitated product is filtered without washing and subsequently dried at 100 °C overnight. The final product was calcined for 5 h at 550 °C with air flow to remove the template. The final solid product is designated as SBA-16.

The catalyst was prepared by the incipient wetness impregnation method. $NiCl_2.6H_2O$ were utilized as the metal sources. Silica gel 60 (comm), silica from rice husk (RHA), and SBA-16 were used as catalyst support. The catalysts were named as Ni/comm, Ni/RHA, and Ni/SBA-16, respectively. Each silica was impregnated with nickel chloride solution (Ni loading = 10 wt%) and followed by the aging process at room temperature for 10 h with periodic stirring. Subsequently, the sample was dried for 10 h at 80 °C and followed by calcination with air flow for 5 h at 450 °C. Finally, the obtained product (Ni/silica) was reduced with H_2 flow at for 5 h 450 °C.

2.3 Characterization of catalyst

X-ray fluorescence (XRF) analysis was carried out using a Bruker S2 PUMA. The X-ray diffraction (XRD) pattern of activated zeolite was obtained by XRD Rigaku Smart Lab with the 2θ angle between 5 and 80°. NH_3-TPD analysis was carried out with a ChemiSorb 2750 Micromeritics to analyze acid strength and the number of acid sites on the catalyst. The surface area and pore size distribution of synthesized catalyst were analyzed by Brunauer-Emmett Teller (BET) Micromeritics TriStar II 3020.

2.4 Catalytic performance

The catalytic reaction was conducted in a high-pressure reactor equipped with a heater and magnetic stirrer. 1 g of oleic acid and 0.1 g of catalyst were added to the reactor. 19 mL of ethanol was used as a solvent. The reactor was purged three times with hydrogen gas. Subsequently, the reactor was filled with hydrogen to 40 bar. The reaction was carried out at 285 °C for 2 h. After the reaction finished, the reactor was cooled to room temperature. Liquid product composition was analyzed using Gas Chromatography-Mass Spectrometry (GC-MS) Agilent 7890A equipped with HP-5MS column.

To determine the remaining amount of oleic acid after reaction and amount of bio-hydrocarbon products, GC-MS area was normalized with eicosane as internal standard. This normalized area from GC-MS analysis is directly proportional to the reactant and product concentration,

$$\text{Normalize Area GC} = \frac{\%\text{Area GC Product}}{\%\text{Area GC Internal Standar}} \times 100\% \quad (1)$$

$$\text{Conversion} = \frac{\text{NA Oleic acid (reactan)} - \text{NAOleic acid (product)}}{\text{NA Oleic acid (reactan)}} \times 100\% \quad (2)$$

$$\text{NA} = \text{Normalized \% Area GC} \quad (3)$$

Table 1
Chemical composition of Ni/silica catalyst

Oxide Type	Weight Percentage (wt%)		
	Ni/Comm	Ni/RHA	Ni/SBA-16
Al_2O_3	1.0	0.6	1.0
MgO	1.5	0.6	1.5
NiO	11.8	17.0	11.5
P_2O_5	0.4	0.7	0.5
SiO_2	84.7	67.3	85.2
Na_2O	-	4.5	-
SO_3	0.2	7.0	0.2
CaO	0.2	0.1	0.1
Cl	0.2	2.3	0.1

3. Result and discussion

3.1 Characterization of catalyst

Chemical composition of Ni/silica in oxide form based on XRF analysis was summarized in Table 1. It can be seen, Ni/RHA contain some impurities, such as Na_2O and SO_3, thus lowering the amount silica in RHA. These impurities may come from RHA itself, but that does not rule out the possibility that these impurities come from the remaining NaOH and H_2SO_4 that were used in RHA preparation. This finding is in line with Park *et al.* who reported that NaOH treatment on RHA may increase the amount of Na_2O (Park *et al.*, 2021).

All prepared catalysts showed three diffraction peaks at 2θ = 44.5°, 51.8°, and 76.3° as shown in Figure 1. This diffraction pattern could be assigned to metallic Ni (111), (200), and (220) plane diffraction line, respectively (JCPDS 04-0850) (Kordouli *et al.*, 2018). There is no other peak corresponding to the nickel crystal phase was observed. This indicates that impregnated nickel was completely reduced to metallic nickel during the reduction process using H_2. Furthermore, two diffraction peaks at 2θ = 32.1° and 48.7° was observed as well in Ni/RHA which could be assigned to Na_2SO_4 (JCPDS 01-074-2036) (Delgadillo-Velasco *et al.*, 2020). The presence of Na_2SO_4 can be attributed to the existence of residual sodium in rice husk that reacts with sulfuric acid during the silica extraction process.

Additionally, NH_3–TPD experiments were conducted to investigate the surface acidity of the catalyst support. In TPD analysis, desorption peak at below 300 °C, in the range 300 °C and 500 °C, and above 500 °C could be categorized as weak, medium, and strong acid, respectively (Wang *et al.*, 2019).

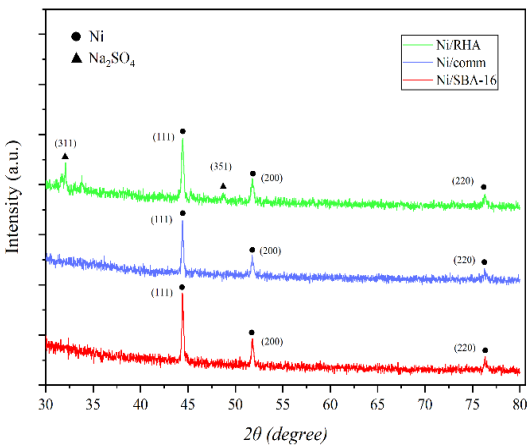

Fig. 1 X-ray diffraction (XRD) diffractogram of Ni/RHA, Ni/comm, and Ni/SBA-16 catalyst

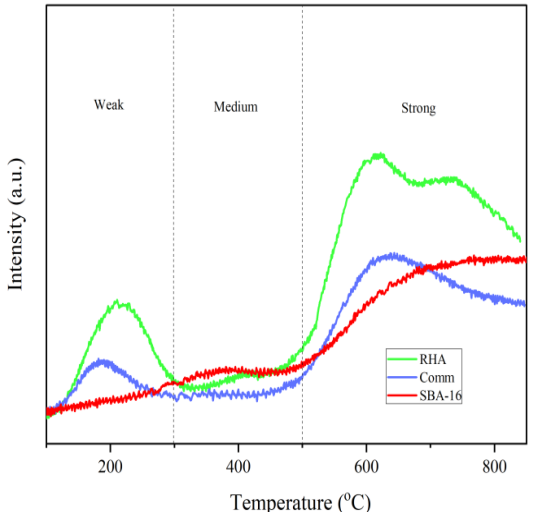

Fig. 2 NH_3-TPD profile of silica

Table 2
Physicochemical properties of the silica support

Catalyst	S_{BET} (m^2/g)	Average Pore Diameter (nm)	Total Acidity (mmol/g)
RHA	192.0	4.05	0.73
SBA-16	799.4	3.42	0.43
Commercial Silica	206.4	6.36	0.45

Figure 2 shows that the surface of all catalyst support is mostly dominated by the presence of strong acid sites, followed by weak acid and a small amount of medium acid sites. Furthermore, among all three catalyst supports, RHA has the highest amount of strong acid sites and highest total acidity as well as shown in Table 2. The most likely explanation for this high acidity is the presence of more impurities in RHA.

The surface area of catalyst support was summarized in Table 2. As expected, SBA-16 has the highest surface area, 799.4 m^2/g. In contrast, RHA has the lowest surface area of 192.0 m^2/g. These results are consistent with previous studies done by Stevens *et al* and Yao *et al.* which reported surface area of 765-989 m^2/g for SBA-16 and 205 m^2/g for RHA. (Stevens *et al.*, 2006; Yao *et al.*, 2016)

The pore size of all three catalysts supports is in the range of 2–50nm, which is classified as mesopores size. In addition, based on pore size distribution as shown in Figure 3, SBA-16 exhibited a narrow distribution of mesopore size of 2.5–3.5 nm,

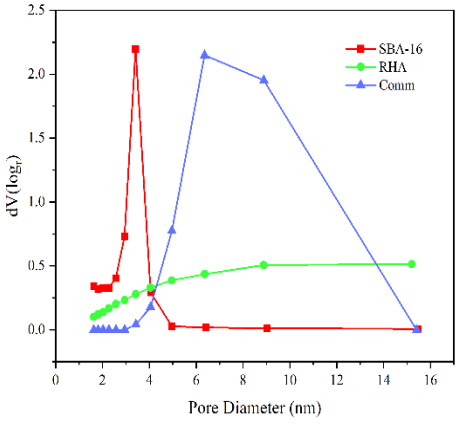

Fig. 3 Pore size distribution of various silica

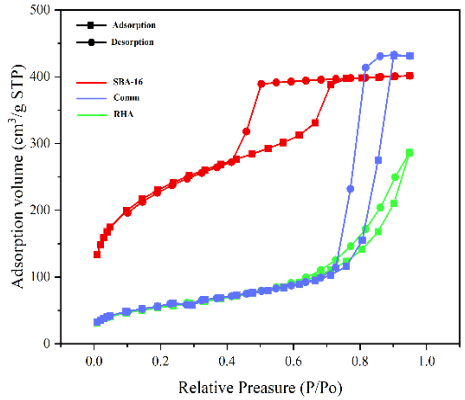

Fig. 4 N_2 adsorption-desorption isotherm of various silica

which indicates that SBA-16 has more ordered pore structure than others. This result is in line with the finding of previous study (Cheng *et al.*, 2003). In contrast, RHA has a wider pore size distribution curve, which indicates that the pore size of RHA is not uniform.

Furthermore, commercial silica showed a wide pore distribution in the range of 5–13 nm. Additionally, all silica showed type IV isotherm as shown in Fig. 4 with hysteresis loop, which is associated with capillary condensation taking place in mesopores (Alothman, 2012). Each silica showed a different type of hysteresis loop, which are type H2, H1, and H3 for SBA-16, commercial silica, and RHA, respectively. Hysteresis type H2 is found primarily in mesoporous materials with uniform cylindrical pore (Cychosz *et al.*, 2018). This result confirms the uniformity of SBA-16 mesopore.

SEM images in Fig. 5 showed the Ni/SBA-16 has spherical particle shape with size in range 3–6 µm. Feliczak-Guzik *et al.* reported SBA-16 has spherical particle shape with particle size in the range of 0.5–8 µm (Feliczak-Guzik *et al.*, 2016). It may be inferred that the particle shape of SBA-16 was preserved upon impregnated with nickel. In contrast with Ni/RHA and Ni/Comm which have more irregular particle shapes.

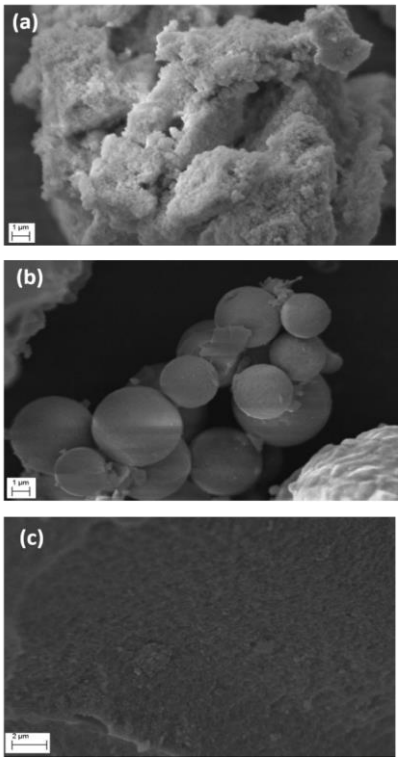

Fig. 5 SEM images of (a) Ni/RHA, (b) Ni/SBA-16, and (c) Ni/Comm

Table 3
Conversion of oleic acid, mass of liquid product, and mass of solid products

Catalyst	Conversion (%)	Liquid Product Mass (gr)	Solid Product Mass (gr)
Ni/RHA	98.25	9.08	2.94
Ni/SBA-16	95.72	11.52	0.85
Ni/Comm	93.76	13.27	0.57

3.2 Catalytic performance

After the reaction finished, both liquid and solid products were obtained. However, in this study only liquid products were analyzed. Table 3 shows that all catalysts exhibited high conversion of oleic acid.

Ni/RHA showed the highest conversion value of 98.25%, followed by Ni/SBA-16 at 95.72% and Ni/comm at 93.76%. Despite the high conversion of oleic acid, the amount of liquid products from the reaction using Ni/RHA is the lowest among other catalysts. The presence of a high amount of acid site in the surface of Ni/RHA may responsible for its high conversion of oleic acid. The presence of acid sites is important in deoxygenation of fatty acids for removal of oxygen in fatty acids via C-O cleavage reaction (Asikin-Mijan *et al.*, 2023). However, the presence of strong acid sites may lead to severe cracking of produced hydrocarbon into shorter hydrocarbon chain with low boiling point. These shorter hydrocarbon chains were in gas phase after the reaction, thus decreasing the number of liquid

Table 4
Variations of deoxygenation products from oleic acid

Catalyst	Normalized % Area GC		
	Ni/RHA	Ni/SBA-16	Ni/Comm
Hydrocarbon Products			
Pentadecane (C15)	0.01	0.01	0.01
Hexadecane (C16)	0.31	0.21	0.20
Heptadecene (C17)	0.03	-	-
Heptadecane (C17)	0.07	0.56	0.02
Octadecene(C18)	4.72	2.32	0.14
Octadecane (C18)	0.61	3.65	2.66
Total Products (C15 - C18)	5.75	6.75	3.03
By-Products			
Fatty Acid Ethyl Ester	5.05	16.19	12.9
Octadecanol	0.18	0.51	0.23
Octadecanal	4.91	0.15	-
Saturated Fatty Acid	-	0.13	0.13
Total By-Products	10.14	16.99	13.26

Table 5
Comparison of present work with other studies

Catalyst	Reaction Condition	Oleic Acid Conversion (%)	Main Product	References
Ni/HZSM-5	320 °C, 40 bar, 5h	47.56	Heptadecene	(Xing *et al*., 2018)
Ni/$CeZrO_2$	300 °C, 1 bar, 3h	98.83	Heptadecane	(Jeon *et al*., 2010)
Surfactant-assisted Synthesis of NiO	300 °C, 20 bar, 3h	100	Heptadecane	(Smoljan *et al*., 2020)
Cu-Ni/ZrO_2	350 °C, 3h	100	Heptadecane	(Zhang *et al*., 2018)
Ni/RHA	285 °C, 40 bar, 2h	98,25	Octadecene	Present work

products. This finding is in accordance with a study by Peng *et al*,-(2012),who reported that increasing the acidity of Ni/HZSM-5 leads to higher conversion of fatty acid but lower selectivity to hydrocarbon due to high acidity promote the cracking of produced alkane (Peng *et al*., 2012). There is also a possibility that shorter hydrocarbons may converted into longer carbon complex through polymerization process, thus increasing the amount of solid products (Asikin-Mijan *et al*., 2017).

The composition of liquid products was summarized in Table 4. Plausible reaction mechanism for hydrodeoxygenation (HDO) starts from hydrogenation of oleic acid into unsaturated fatty acid, stearic acid and then, hydrogenation of stearic acid into octadecanol and followed by dehydration of octadecanol, which leads to octadecene formation.

Furthermore, in the decarbonylation pathway, the removal of oxygen atoms through hydrogenation of the hydroxyl group of stearic acid and followed by the removal of carbonyl group, leads to heptadecene, carbon monoxide and water formation. Additionally, in the decarboxylation pathway, two oxygen atoms of carboxylic acid group of stearic acid are removed, causing the formation of heptadecane and carbon dioxide (Wu *et al*., 2018). Furthermore, pentadecane and hexadecane products may form due to cracking reaction of C17 and C18 (Žula *et al*., 2022). Table 4 also depicts that all catalysts exhibited the hydrodeoxygenation (HDO) reaction as the main reaction pathway. This is indicated by the presence of C18 (octadecene and octadecane) with the highest amount among other hydrocarbon products. Decarboxylation product, heptadecane was obtained as well in reaction using all catalysts. In contrast, the decarbonylation reaction pathway is only observed in the reaction using Ni/RHA, which indicates by the presence of heptadecene. Highest amount of hexadecane was observed in the reaction using Ni/RHA. This result indicates that more cracking reaction occurred when Ni/RHA is used, which may be caused by high acidity of Ni/RHA (Zhang *et al*., 2019).

Additionally, fatty acid ethyl ester (FAEE) was observed as by products in all three catalysts. It is hypothesized that esterification of fatty acid with the solvent ethanol may occurred, resulted the formation of FAEE. Ni metal is able to catalyze an esterification of fatty acid (carboxylic acid) with alcohol (Liu *et al*., 2023).

Table 5 compares conversion and main product results from the present study with other research works. The low oleic acid conversion of 47.56% was obtained from the reaction at 320 °C with reaction time of 5h. Additionally, heptadecene was obtained as the main product, which indicates that the dominant reaction pathway is decarbonylation (Xing *et al*., 2018). Three other studies exhibited higher conversion of oleic acid in the range of 98.83%-100% with heptadecane as the main product. The presence of heptadecane indicated decarboxylation is the primary reaction pathway (Jeon *et al*., 2010; Smoljan *et al*., 2020; Zang *et al*., 2018). In this present work, a conversion of 98.25% was obtained with a lower reaction temperature and shorter reaction time compared to other works. Furthermore, octadecene was obtained as main product, which indicates that hydrodeoxygenation is the dominant reaction pathway.

4. Conclusions

Rice husk can be used as a silica source and utilized as catalyst support for nickel catalyst in synthesis of biohydrocarbon from deoxygenation of oleic acid. Different sources of silica resulted in different properties of Ni/silica catalyst. Ni/RHA showed the highest oleic acid conversion of 98.25%, followed by Ni/SBA-16 at 95.72% and Ni/comm at 93.76%. Ni/RHA has the highest amount of acid sites compare to Ni/comm and Ni/SBA-16. Higher acidity of Ni/RHA leads to higher conversion of oleic acid. But excessive acidity tends to promote catalytic cracking, thus produce shorter hydrocarbon instead of C15-C18 hydrocarbon. Therefore, Ni/RHA has the highest conversion of oleic acid but the smallest number of liquid products. In terms of deoxygenation reaction pathway to produce hydrocarbon, hydrodeoxygenation and decarboxylation pathway were observed in the reaction using all three catalysts. Decarbonylation pathway was only observed in the reaction using Ni/RHA. Furthermore, Ni/SBA-16, a catalyst with moderate acidity and highest surface area exhibited the highest yield of C15-C18 hydrocarbon compare to other catalysts, Ni/RHA and Ni/Comm.

Acknowledgments

The authors express their gratitude to Collaborative STEM Laboratories (CSL), Universitas Prasetiya Mulya for the support in accomplishing this research.

Author Contributions: R.R.: Conceptualization, methodology, experimentation, formal analysis, writing—original draft, N.R.; writing—review and editing, R.T.Y.; writing—review and editing, A.A.D.; Conceptualization, methodology, supervision, resources, formal analysis, F.S.H.S.; methodology, supervision, resources, formal analysis, writing—original draft. All authors have read and agreed to the published version of the manuscript.

Funding: This research was funded by Korea Institute of Science and Technology (KIST) School Project Grant.

Conflicts of Interest: The authors declare no conflict of interest.

References

ALOthman, Z. A. (2012). A review: fundamental aspects of silicate mesoporous materials. *Materials,* 5(12), 2874-2902. https://doi.org/10.3390/ma5122874

Asikin-Mijan, N., Juan, J. C., Taufiq-Yap, Y. H., Ong, H. C., Lin, Y. C., AbdulKareem-Alsultan, G., & Lee, H. V. (2023). Towards sustainable green diesel fuel production: Advancements and opportunities in acid-base catalyzed H2-free deoxygenation process. *Catalysis Communications,* 182, 106741. https://doi.org/10.1016/j.catcom.2023.106741

Asikin-Mijan, N., Lee, H. V., Abdulkareem-Alsultan, G., Afandi, A., & Taufiq-Yap, Y. H. (2017). Production of green diesel via cleaner catalytic deoxygenation of Jatropha curcas oil. *Journal of Cleaner Production*, *167*, 1048-1059. https://doi.org/10.1016/j.jclepro.2016.10.023

Chaudhary, V., & Sharma, S. (2017). An overview of ordered mesoporous material SBA-15: synthesis, functionalization and application in oxidation reactions. Journal of Porous Materials, 24, 741-749. https://doi.org/10.1007/s10934-016-0311-z

Chen, K. T., Wang, J. X., Dai, Y. M., Wang, P. H., Liou, C. Y., Nien, C. W., ... & Chen, C. C. (2013). Rice husk ash as a catalyst precursor for biodiesel production. *Journal of the Taiwan Institute of Chemical Engineers*, 44(4), 622-629. http://dx.doi.org/10.1016/j.jtice.2013.01.006

Chang, F. W., Yang, H. C., Roselin, L. S., & Kuo, W. Y. (2006). Ethanol dehydrogenation over copper catalysts on rice husk ash prepared by ion exchange. *Applied Catalysis A: General*, 304, 30-39. https://doi.org/10.1016/j.apcata.2006.02.017

Cheng, C. F., Lin, Y. C., Cheng, H. H., & Chen, Y. C. (2003). The effect and model of silica concentrations on physical properties and particle sizes of three-dimensional SBA-16 nanoporous materials. Chemical physics letters, 382(5-6), 496-501. https://doi.org/10.1016/j.cplett.2003.10.122

Cychosz, K. A., & Thommes, M. (2018). Progress in the physisorption characterization of nanoporous gas storage materials. Engineering, 4(4), 559-566. https://doi.org/10.1016/j.eng.2018.06.001

De, S., Zhang, J., Luque, R., & Yan, N. (2016). Ni-based bimetallic heterogeneous catalysts for energy and environmental applications. *Energy & environmental science*, 9(11), 3314-3347. https://doi.org/10.1039/c6ee02002j

Delgadillo-Velasco, L., Hernández-Montoya, V., Montes-Morán, M. A., Gómez, R. T., & Cervantes, F. J. (2020). Recovery of different types of hydroxyapatite by precipitation of phosphates of wastewater from anodizing industry. *Journal of cleaner production*, 242, 118564. https://doi.org/10.1016/j.jclepro.2019.118564

Feliczak-Guzik, A., Jadach, B., Piotrowska, H., Murias, M., Lulek, J., & Nowak, I. (2016). Synthesis and characterization of SBA-16 type mesoporous materials containing amine groups. *Microporous and Mesoporous Materials*, 220, 231-238. http://dx.doi.org/10.1016/j.micromeso.2015.09.006

Jeon, K. W., Na, H. S., Lee, Y. L., Ahn, S. Y., Kim, K. J., Shim, J. O., Jang, W.J., Jeong, D.W., Nah, I.W., & Roh, H. S. (2019). Catalytic deoxygenation of oleic acid over a Ni-CeZrO2 catalyst. *Fuel,* 258, 116179. https://doi.org/10.1016/j.fuel.2019.116179

Kaewtrakulchai, N., Smuthkochorn, A., Manatura, K., Panomsuwan, G., Fuji, M., & Eiad-Ua, A. (2022). Porous biochar supported transition metal phosphide catalysts for hydrocracking of palm oil to bio-jet fuel. *Materials*, 15(19), 6584. https://doi.org/10.3390/ma15196584

Kamaruzaman, M. F., Taufiq-Yap, Y. H., & Derawi, D. (2020). Green diesel production from palm fatty acid distillate over SBA-15-supported nickel, cobalt, and nickel/cobalt catalysts. *Biomass and bioenergy*, *134*, 105476. https://doi.org/10.1016/j.biombioe.2020.105476

Karam, L., & El Hassan, N. (2018). Advantages of mesoporous silica based catalysts in methane reforming by CO2 from kinetic perspective. *Journal of Environmental Chemical Engineering*, 6(4), 4289-4297. https://doi.org/10.1016/j.jece.2018.06.031

Katiyar, A., Yadav, S., Smirniotis, P. G., & Pinto, N. G. (2006). Synthesis of ordered large pore SBA-15 spherical particles for adsorption of biomolecules. *Journal of Chromatography A*, 1122(1-2), 13-20. https://doi.org/10.1016/j.chroma.2006.04.055

Kordouli, E., *et al.* "Hydrodeoxygenation of Phenol on Bifunctional Ni-Based Catalysts: Effects of Mo Promotion and Support." *Applied Catalysis B: Environmental*, vol. 238, 2018, pp. 147–60, https://doi.org/10.1016/j.apcatb.2018.07.012

Liu, C., Marhaba, M., Dilshat, A., Zhu, W., Xia, K., Mao, Z., & Ablimit, A. (2023). Nickel-catalyzed esterification of mandelic acids with alcohols. *Arabian Journal of Chemistry,* 16(1), 104407. https://doi.org/10.1016/j.arabjc.2022.104407

Liu, J., Li, C., Wang, F., He, S., Chen, H., Zhao, Y., ... & Duan, X. (2013). Enhanced low-temperature activity of CO 2 methanation over highly-dispersed Ni/TiO 2 catalyst. *Catalysis Science & Technology,* 3(10), 2627-2633. https://doi.org/10.1039/c3cy00355h

Liu, S., Zhu, Q., Guan, Q., He, L., & Li, W. (2015). Bio-aviation fuel production from hydroprocessing castor oil promoted by the nickel-based bifunctional catalysts. *Bioresource technology*, 183, 93-100. https://doi.org/10.1016/j.biortech.2015.02.056

Muanruksa, P., Wongsirichot, P., Winterburn, J., & Kaewkannetra, P. (2021). Integrated cleaner biocatalytic process for biodiesel production from crude palm oil comparing to refined palm oil. *Catalysts,* 11(6), 734. https://doi.org/10.3390/catal11060734

Ogwang, G., Olupot, P. W., Kasedde, H., Menya, E., Storz, H., & Kiros, Y. (2021). Experimental evaluation of rice husk ash for applications in geopolymer mortars. *Journal of Bioresources and Bioproducts,* 6(2), 160-167. https://doi.org/10.1016/j.jobab.2021.02.008

Oi, L. E., Choo, M. Y., Lee, H. V., Ong, H. C., Abd Hamid, S. B., & Juan, J. C. (2016). Recent advances of titanium dioxide (TiO 2) for green organic synthesis. *Rsc Advances*, 6(110), 108741-108754. https://doi.org/10.1039/c6ra22894a

Ooi, X. Y., Gao, W., Ong, H. C., Lee, H. V., Juan, J. C., Chen, W. H., & Lee, K. T. (2019). Overview on catalytic deoxygenation for biofuel synthesis using metal oxide supported catalysts. *Renewable and Sustainable Energy Reviews*, 112, 834-852. https://doi.org/10.1016/j.rser.2019.06.031

Park, J. Y., Gu, Y. M., Park, S. Y., Hwang, E. T., Sang, B. I., Chun, J., & Lee, J. H. (2021). Two-stage continuous process for the extraction of silica from rice husk using attrition ball milling and alkaline leaching methods. *Sustainability,* 13(13), 7350. https://doi.org/10.3390/su13137350

Paviotti, M. A., Hoyos, L. A. S., Busilacchio, V., Faroldi, B. M., & Cornaglia, L. M. (2020). Ni mesostructured catalysts obtained from rice husk ashes by microwave-assisted synthesis for CO2 methanation. *Journal of CO_2 Utilization*, 42, 101328. https://doi.org/10.1016/j.jcou.2020.101328

Peng, B., Yao, Y., Zhao, C., & Lercher, J. A. (2012). Towards quantitative conversion of microalgae oil to diesel-range alkanes with bifunctional catalysts. *Angewandte Chemie-International Edition,* 51(9), 2072. https://doi.org/10.1002/anie.201106243

Rashidi, N. A., Mustapha, E., Theng, Y. Y., Razak, N. A. A., Bar, N. A., Baharudin, K. B., & Derawi, D. (2022). Advanced biofuels from waste cooking oil via solventless and hydrogen-free catalytic deoxygenation over mesostructured Ni-Co/SBA-15, Ni-Fe/SBA-15, and Co-Fe/SBA-15 catalysts. *Fuel*, 313, 122695. https://doi.org/10.1016/j.fuel.2021.122695

Richardson, J. T., Scates, R., & Twigg, M. V. (2003). X-ray diffraction study of nickel oxide reduction by hydrogen. *Applied Catalysis A: General*, 246(1), 137-150. https://doi.org/10.1016/S0926-860X(02)00669-5

Smoljan, C. S., Crawford, J. M., & Carreon, M. A. (2020). Mesoporous microspherical NiO catalysts for the deoxygenation of oleic acid. *Catalysis Communications*, 143, 106046. https://doi.org/10.1016/j.catcom.2020.106046

Stevens, W. J., Lebeau, K., Mertens, M., Van Tendeloo, G., Cool, P., & Vansant, E. F. (2006). Investigation of the morphology of the mesoporous SBA-16 and SBA-15 materials. *The Journal of Physical Chemistry B*, 110(18), 9183-9187. https://doi.org/10.1021/jp0548725

Syed-Hassan, Syed Shatir A., and Chun Zhu Li. "NiO Reduction with Hydrogen and Light Hydrocarbons: Contrast between SiO2-Supported and Unsupported NiO Nanoparticles." *Applied Catalysis A: General*, vol. 398, no. 1–2, 2011, pp. 187–94, https://doi.org/10.1016/j.apcata.2011.03.033

Takahashi, R., Sato, S., Sodesawa, T., Kawakita, M., & Ogura, K. (2000). High surface-area silica with controlled pore size prepared from nanocomposite of silica and citric acid. *The Journal of Physical*

Chemistry B, 104(51), 12184-12191. https://doi.org/10.1021/jp002662g

Wang, N., Feng, Y., Chen, Y., & Guo, X. (2019). Lithium-based sorbent from rice husk materials for hydrogen production via sorption-enhanced steam reforming of ethanol. *Fuel*, 245, 263-273. https://doi.org/10.1016/j.fuel.2019.02.048

Wang, Y., Craven, M., Yu, X., Ding, J., Bryant, P., Huang, J., & Tu, X. (2019). Plasma-enhanced catalytic synthesis of ammonia over a Ni/Al2O3 catalyst at near-room temperature: insights into the importance of the catalyst surface on the reaction mechanism. *ACS catalysis*, 9(12), 10780-10793., https://doi.org/10.1021/acscatal.9b02538

Wu, G., Zhang, N., Dai, W., Guan, N., & Li, L. (2018). Construction of bifunctional Co/H-ZSM-5 catalysts for the hydrodeoxygenation of stearic acid to diesel-range alkanes. *ChemSusChem*, 11(13), 2179-2188. https://doi.org/10.1002/cssc.201800670

Xing, S., Lv, P., Zhao, C., Li, M., Yang, L., Wang, Z., Chen, Y., & Liu, S. (2018). Solvent-free catalytic deoxygenation of oleic acid via nano-Ni/HZSM-5: Effect of reaction medium and coke characterization. *Fuel processing technology*, 179, 324-333. https://doi.org/10.1016/j.fuproc.2018.07.024

Yao, X., Xu, K., & Liang, Y. (2016). Comparing the thermo-physical properties of rice husk and rice straw as feedstock for thermochemical conversion and characterization of their waste ashes from combustion. *BioResources*, 11(4), 10549-10564. https://doi.org/10.15376/biores.11.4.10549-10564

Zhang, J., Chen, T., Jiao, Y., Wang, L., Wang, J., Chen, Y., Zhu, Q., & Li, X. (2020). Role of acidity in catalytic cracking of n-decane over supported Pt-based catalysts. *Applied Surface Science*, 507, 145113. https://doi.org/10.1016/j.apsusc.2019.145113

Zhang, Z., Chen, H., Wang, C., Chen, K., Lu, X., Ouyang, P., & Fu, J. (2018). Efficient and stable Cu-Ni/ZrO2 catalysts for in situ hydrogenation and deoxygenation of oleic acid into heptadecane using methanol as a hydrogen donor. *Fuel*, 230, 211-217. https://doi.org/10.1016/j.fuel.2018.05.018

Žula, M., Grilc, M., & Likozar, B. (2022). Hydrocracking, hydrogenation and hydro-deoxygenation of fatty acids, esters and glycerides: Mechanisms, kinetics and transport phenomena. *Chemical Engineering Journal*, 444, 136564. https://doi.org/10.1016/j.cej.2022.136564